

Freezing of spin and charge in  $\text{La}_{2-x}\text{Sr}_x\text{CuO}_4$ 

D. R. Harshman, G. Aeppli, G. P. Espinosa, A. S. Cooper, and J. P. Remeika  
*AT&T Bell Laboratories, Murray Hill, New Jersey 07974*

E. J. Ansaldo  
*University of Saskatchewan, Saskatoon, Canada S7N0K3*

T. M. Riseman and D. Ll. Williams  
*University of British Columbia, Vancouver, British Columbia Canada V6T2A6*

D. R. Noakes  
*Atomic Energy of Canada Ltd., Chalk River Nuclear Laboratories, Chalk River, Ontario, Canada K0J1J0*

B. Ellman and T. F. Rosenbaum  
*University of Chicago, Chicago, Illinois 60637*  
 (Received 14 January 1988)

Zero- and longitudinal-field muon-spin relaxation ( $\mu^+$ SR) measurements have been performed on  $\text{La}_{2-x}\text{Sr}_x\text{CuO}_4$  alloys in both single-crystal and sintered powder forms above and below their magnetic transition temperatures,  $T_f$ . The  $\mu^+$  precession frequency  $\nu$  depends only weakly on  $x$  and  $T_f$ , an observation which together with resistivity data implies classical freezing of magnetic moments in the regime where the carriers are localized. For  $x=0.05$ , critical dynamics are observed near  $T_f$ . The  $\mu^+$ SR technique is shown to be very sensitive to ferromagnetically aligned pairs of  $\text{Cu}^{2+}$  moments; the population of such pairs increases greatly with  $x$ .

Over the past year or so, various cuprates have been found to be superconducting with transition temperatures ( $T_c$ 's) as high as  $\sim 90$  K.<sup>1</sup> Bulk investigations of related compounds,<sup>2</sup> such as  $\text{La}_2\text{CuO}_{4-\delta}$ , have also been performed in the hope that they may provide a basis for understanding the superconducting materials. Neutron scattering experiments have confirmed the existence of antiferromagnetism and its sensitivity to oxygen stoichiometry in  $\text{La}_2\text{CuO}_{4-\delta}$ .<sup>3</sup> In the present paper, we describe a detailed study of magnetic order in the  $\text{La}_{2-x}\text{Sr}_x\text{CuO}_4$  series, precursors to the superconducting systems that are obtained for  $x \geq 0.06$ . We have chosen to use the muon-spin relaxation ( $\mu^+$ SR) technique because the results obtained are relatively simple to interpret, giving a direct measure of the internal fields in bulk samples. This technique is also sensitive to fluctuations in the internal field, yielding information on the dynamical evolution of the magnetic moments in the sample.

Single-crystal  $\text{La}_2\text{CuO}_4$  samples with dimensions  $2 \times 2 \times 0.5$  mm<sup>3</sup> were mounted on an aluminum backing such that the incident  $\mu^+$  momentum was orthogonal to the plates (i.e., parallel to the tetragonal  $c$  axis). Sintered powder samples (disks), roughly 2.5 cm diameter and 3 mm thick, were mounted similarly on the cold finger of a <sup>4</sup>He cryostat. The resistivity  $\rho$  is shown as a function of temperature in Fig. 1 for  $x=0.02$ , indicating that this sample is metallic to 100 K, below which  $\rho$  increases with decreasing temperature; for  $0.3 < T < 8$  K, the resistivity follows the law  $\rho \sim \exp(T_0/T)^{1/2}$ , where  $T_0 \approx 74$  K. Note that these data are very similar to data taken for single crystals<sup>4</sup> of the type also used in the present study.

The time-differential  $\mu^+$ SR technique used here is de-

scribed elsewhere<sup>5</sup> so only a brief discussion will be given. Energetic (4.2 MeV) positive muons ( $\mu^+$ ) are stopped in the sample where they decay, emitting a positron preferentially along their final spin polarization. A clock is started when the incident muon enters the sample and stopped upon the subsequent detection of the decay positron. Because the muons are created (via pion decay) with spin antiparallel to their momentum, the time evolution of the  $\mu^+$  spin can be observed. Typically, one mea-

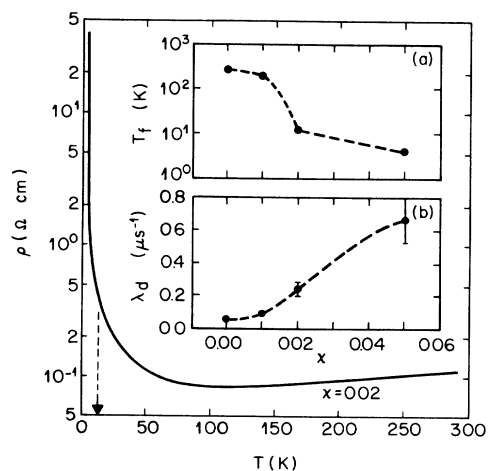


FIG. 1. Resistivity for  $x=0.02$ ; the arrow indicates the magnetic freezing transition for this sample. The inset shows  $x$  dependence of the (a) magnetic freezing (Néel) temperatures and (b) decay rates  $\lambda_d$  for sintered  $\text{La}_{2-x}\text{Sr}_x\text{CuO}_4$ . The dashed lines are guides to the eye.

sures the spin orientations of millions of muons, one at a time, yielding an ensemble average,  $G_{zz}(t)$ . Standard magnetic field geometries allow the application of fields in various directions relative to the initial  $\mu^+$  polarization. In the present work, mainly zero- and longitudinal-field measurements were made, which typically yield a  $T_1$ -type relaxation function, or, as in the case of three-dimensional antiferromagnetic (AFM) ordering, a precessing signal with a  $T_2$  relaxation due to inhomogeneous broadening.

Figure 2 shows zero-field data taken for sintered  $\text{La}_{2-x}\text{Sr}_x\text{CuO}_4$ , with  $x=0, 0.01, 0.02$ , and  $0.05$ . Spectra taken at the lowest temperatures are on the right side of the figure; the damped oscillations observed are due to muon-spin precession in frozen local fields.<sup>6</sup> We emphasize that  $\mu^+$  SR is sensitive only to local fields, so that unless other information is available, a true Néel state cannot be distinguished from a state without long-range AFM order but with local moments frozen on the time scale ( $\sim 5 \mu\text{s}$ ) of the  $\mu^+$  SR experiment. The muon-spin precession frequency  $\nu$  and damping rate  $1/T_2$  are directly proportional to the average local field  $\bar{H}$  and some typical deviation  $\Delta$  of the local field from  $\bar{H}$ , respectively, with the constant of proportionality equal to the gyromagnetic ratio of the muon,  $\gamma_\mu = 2\pi \times 13.55 \text{ MHz/kG}$ . The AFM precession frequency  $\nu$  is plotted as a function of temperature for the sintered powder samples with strontium concentra-

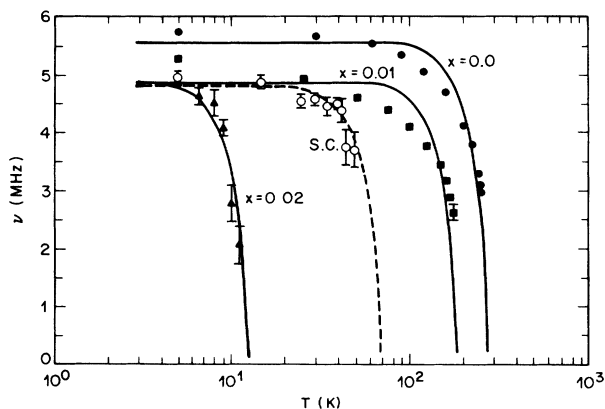


FIG. 3. The muon Larmor precession frequency  $\nu$  plotted as a function of temperature for sintered  $\text{La}_{2-x}\text{Sr}_x\text{CuO}_4$  and single-crystal (s.c.)  $\text{La}_2\text{CuO}_4$ .

tions of 0, 0.01, and 0.02 in Fig. 3. Data are also shown for the single-crystal  $\text{La}_2\text{CuO}_4$  sample. The most striking observation is the dramatic decrease in the spin-freezing temperature  $T_f$  associated with relatively small increases in  $x$  [see inset (a) in Fig. 1]. Data for  $x=0.05$  are not shown in Fig. 3 because this sample displays magnetic freezing at  $4 \pm 1 \text{ K}$ , which is near the lower temperature

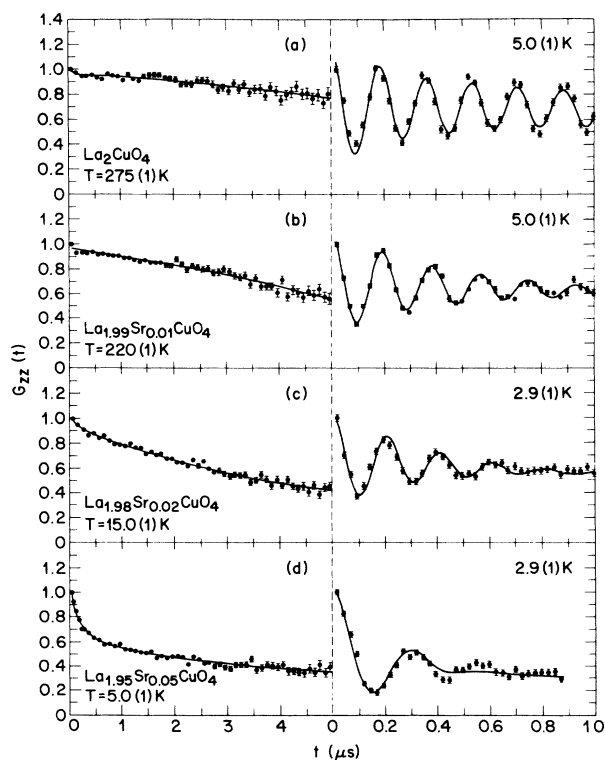


FIG. 2. Summary of zero-field data above and below  $T_f$  for sintered (a)  $\text{La}_2\text{CuO}_4$  at 275(1) K and 5.0(1) K, (b)  $\text{La}_{1.99}\text{Sr}_{0.01}\text{CuO}_4$  at 220(1) K and 5.0(1) K, (c)  $\text{La}_{1.98}\text{Sr}_{0.02}\text{CuO}_4$  at 15.0(1) K and 2.9(1) K, and (d)  $\text{La}_{1.95}\text{Sr}_{0.05}\text{CuO}_4$  at 5.0(1) K and 2.9(1) K. The lines through the data are fits assuming the function described in the text.

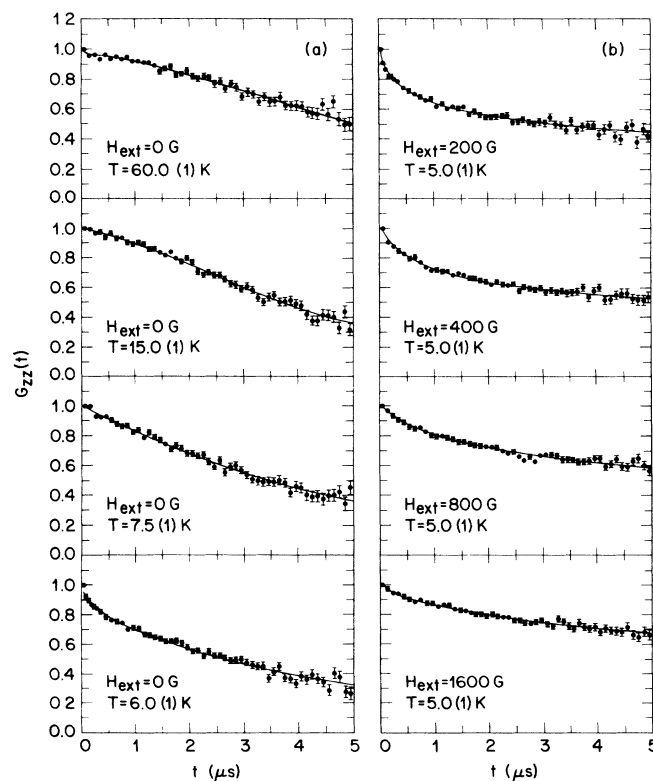


FIG. 4. Zero- and longitudinal-field data for sintered  $\text{La}_{1.95}\text{Sr}_{0.05}\text{CuO}_4$ . Frame (a) shows the temperature dependence of the relaxation signal, while (b) shows the decoupling of the relaxation at 5.0(1) K. The lines through the data are fits assuming the function described in the text.

limit achievable in our cryostat. The solid lines through the data are fits assuming the mean-field approximation below  $T_f$ . Note that at low temperatures, the frequencies for all  $x \leq 0.02$  approach a value of  $\sim 5.5$  MHz; for  $x = 0.05$ , the fitted  $\nu$  at 2.9(1) K is  $\sim 3.4$  MHz (this relatively lower value is due to the close proximity of 2.9 K to  $T_f$ ). Thus, the frozen magnetic moment in  $\text{La}_{2-x}\text{Sr}_x\text{CuO}_4$  is essentially independent of  $x$  for  $x \leq 0.05$ , even though the freezing (Néel) temperature varies by almost two orders of magnitude. It is also independent of whether the samples are conventional powders or (PbO) flux-grown single crystals (the comparatively low  $T_f$  observed for the single crystals probably arises from Pb substituted for La).<sup>4</sup> Other workers have obtained the same result for  $\text{La}_2\text{CuO}_{4-\delta}$ , where the Néel temperature is varied by changing  $\delta$ .<sup>7</sup> In contrast to  $\bar{H}$ ,  $\Delta$  depends strongly on  $x$ . This result is clear from Fig. 2, which shows that the envelope of the muon precession signal decays most rapidly for large  $x$ , indicating that the internal field becomes more inhomogeneous as Sr is introduced.

Inspection of the left-hand column of Fig. 2 shows that increases in the Sr content also yield dramatic changes in the  $\mu^+$ SR at temperatures slightly above  $T_f$ . In particular, the initial muon depolarization rate is largest for the magnetic sample with the largest Sr content ( $x = 0.05$ ). Because the depolarization rate is—as in NMR—inversely proportional to the magnetic relaxation rate for the electronic moments in the sample, the spins in the more metallic samples relax at a considerably lower rate prior to freezing, when they produce a static field wherein the muons can precess. Figure 4(a) shows that as the temperature is raised for  $x = 0.05$ , the initial depolarization rate decreases rapidly, as it should for conventional critical slowing down near a second-order transition to a frozen state.<sup>5,8</sup>

To obtain further information about the magnetic dynamics, we performed measurements with an external

field ( $H_{\text{ext}}$ ) applied parallel to initial muon-spin direction. Figure 4(b) shows the  $\mu^+$ SR results for various longitudinal fields applied to sintered  $\text{La}_{1.95}\text{Sr}_{0.05}\text{CuO}_4$  at 5.0(1) K [see Fig. 2(d) for corresponding zero-field data]. As is apparent, a field of order 400 G is needed to largely eliminate the initial decay which we associate with critical fluctuations. Not surprisingly, 400 G compares well with the internal field established from the muon precession observed in the low-temperature, frozen-moment state. What is more unusual, is that even for the largest field (1600 G) applied, a substantial decay of  $G_{zz}(t)$  with time persists. Indeed, Fig. 4 strongly suggests that  $G_{zz}(t)$  is the sum of two components: one derived from magnetic fluctuations which freeze to yield muon-spin precession at low temperatures, and another due to a set of apparently stronger moments which do not yield a precession signal. A multicomponent  $\mu^+$ SR signal arises naturally when there are different muon sites in the sample. In oxides, one expects positive muons to be attracted to the negatively charged oxygen ions. For  $\text{La}_2\text{CuO}_4$ , there are two types of oxygen sites, namely those (type I) providing superexchange paths within the  $\text{CuO}_2$  planes and those (type II) between the planes, each closest to a unique  $\text{Cu}^{2+}$  ion. Muons located at the planar bonding oxygens will, in the AFM phase, be exposed to zero field by virtue of the cancellation of contributions from the two Néel sublattices. By the same token, they are very sensitive to disturbances where the spins on neighboring copper ions are parallel. In contrast, muons near type-II oxygens experience a non-zero local field due to the local moments on the  $\text{Cu}^{2+}$  sites, independent of the relative orientation of neighboring moments. Owing to the random orientation of the sintered powders, a proper description of the time evolution of the  $\mu^+$  spin is obtained by performing a powder average of precession signals for an ordered magnet. Assuming a Gaussian distribution of internal fields, one obtains the zero-field relaxation function

$$G_{zz}(t) = \frac{1}{\sqrt{8\pi}} \int_0^\pi \int_{-\infty}^\infty \sin\theta [\cos^2\theta + \sin^2\theta \cos(\gamma_\mu H t \sin\theta)] \exp\left[-\frac{(\bar{H}-H)^2}{2\Delta^2}\right] d\left[\frac{H}{\Delta}\right] d\theta. \quad (1)$$

The lines through the data in Figs. 2 and 4 are the results of fits assuming a relaxation function derived from the normalized sum of Eq. (1), or its paramagnetic (dynamic) analogue,<sup>8</sup> and a nonprecessing background term (with approximately equal weightings). As is evident from Fig. 2, this function provides an excellent description of all data except for those obtained for the frozen spin state with  $x = 0.05$ , the failure likely due to the close proximity of 2.9 K to  $T_f$ . The fitted values for  $\gamma_\mu\Delta$  are 0.001 and 0.36 MHz for  $x = 0$  and 0.02, respectively, confirming the dramatic increase in internal field inhomogeneity with increasing  $x$ . The long-time (exponential) decay rate  $\lambda_d$  of the background signal, associated with the muons located near the planar oxygens, also increases with  $x$  as shown in inset (b) of Fig. 1. Thus as  $x$  is increased, the lifetime of triplets formed from neighboring copper spins increases, or indistinguishably, the spin-wave velocity decreases.

An important conclusion of our experiments is that the internal field at low temperatures is essentially indepen-

dent of the Sr concentration and nominal ordering temperature  $T_f$ , as has also been found for  $\text{La}_2\text{CuO}_{4-\delta}$ .<sup>6,7</sup> At the same time, our data show that the inhomogeneity in the local field increases greatly with  $x$ , as does the extent (measured by  $\lambda_d$ ) to which nearest-neighbor spins are parallel. Furthermore, neutron-diffraction measurements show that the three-dimensional (3D) ordered moment decreases rapidly with  $T_f$ .<sup>3</sup> The explanation for this behavior lies in the fact that the muon is a local probe, while the neutron diffraction technique measures the staggered magnetization. Thus, our  $\mu^+$ SR measurements together with the available neutron diffraction data indicate that for larger  $x$  and smaller  $\delta$ , spin-glass ordering takes the place of antiferromagnetism. We suggest that the crossover between the two types of behavior occurs where the  $x$  dependence of the ordering temperature changes from rapid to gentle, i.e., for  $x \approx 0.02$  (see inset of Fig. 1). Guided also by the precedent set by random magnetic alloys such as  $\text{Eu}_{1-x}\text{Sr}_x\text{S}$  and  $(\text{Fe}_{1-x}\text{Mn}_x)_{75}\text{P}_{16}\text{B}_6\text{Al}_3$ ,<sup>9</sup> we

anticipate reentrant spin-glass (RSG) behavior in antiferromagnetic samples. RSG phenomena may well account for some of the lower-temperature anomalies found by susceptibility, nuclear resonance techniques, and neutron scattering in materials based on  $\text{La}_2\text{CuO}_4$ .<sup>10</sup>

Spin-glass behavior generally arises from random competing interactions. Such interactions occur quite naturally in  $\text{La}_{2-x}\text{Sr}_x\text{CuO}_4$  if the holes introduced by the substitution are situated on the oxygens forming the bonds between copper ions.<sup>11</sup> Several workers<sup>12</sup> have pointed out that if localized, these holes will yield a net ferromagnetic exchange interaction between the neighboring  $\text{Cu}^{2+}$  ions. Our result that as  $x$  is increased, there is a growing relaxation rate ( $\lambda_d$ ) for muons at type-I sites, represents perhaps the most direct evidence for the introduction of such interactions. For very small  $x$ , the ferromagnetic links in the  $\text{Cu}^{2+}$  lattice are sufficiently sparse that AFM order will survive, while for large  $x$ , spin-glass order will occur; in the intermediate regime, we expect RSG behavior.

Motivated by the result that the frozen moment strength in  $\text{La}_{2-x}\text{Sr}_x\text{CuO}_4$  is essentially independent of  $x$ , we have described how 3D magnetic freezing can occur for  $\text{La}_2\text{CuO}_4$ -based materials. This result also implies that at zero temperature, Sr substitution does not introduce moment-reducing quantum fluctuations more significant than those (spin waves) present for  $x=0$ . In other words, the zero-temperature magnetic phase transition presumed to occur for  $x=x_c$  with  $0.05 < x_c < 0.15$  could well be of first order, driven by a reduction in the effective exchange coupling  $J_{\text{eff}}$  to zero at  $x_c$ . That  $J_{\text{eff}}$  is a strong function of  $x$  is apparent from the reduction of  $T_f$  with  $x$

and the simultaneously increasing visibility (see insets of Fig. 1) of magnetic fluctuations in our  $\mu^+$ SR experiments. We also note that inelastic neutron scattering has shown that excess oxygen dramatically reduces the spin-wave velocity ( $c \sim J_{\text{eff}}$ ) of  $\text{La}_2\text{NiO}_4$ ,<sup>13</sup> a system very similar to  $\text{La}_2\text{CuO}_4$ .

In addition to finding classical spin-glass-like behavior in the more heavily substituted materials, we have found that in the same materials, the resistivity has a minimum at intermediate temperatures, followed by a low-temperature upturn characteristic of disordered systems with strong Coulomb interactions,<sup>14</sup>  $\rho \sim \exp(T_0/T)^{1/2}$ . The magnetic freezing for the more heavily substituted samples occurs at temperatures well within the latter regime, which suggests that carrier localization—most likely near the planar oxygens—is a prerequisite for the spin-freezing transition. Thus, contrary to statements made by others,<sup>7</sup> ideas borrowed from experience with itinerant magnetism are not applicable to  $\text{La}_{2-x}\text{Sr}_x\text{CuO}_4$ . It is probably more appropriate to imagine that as the Sr content is increased, there is a crossover from insulating antiferromagnetism to Coulomb glass behavior, the latter involving a freeze-out of both magnetic and charge degrees of freedom.

We thank K. Hoyle, R. Keitel, and J. Worden for technical assistance. We also acknowledge helpful discussions with J. H. Brewer, Z. Fisk, P. Littlewood, D. Monroe, and C. M. Varma. Research at TRIUMF and University of Chicago are supported by the Natural Sciences and Engineering Research Council of Canada and National Science Foundation Grant No. DMR-85-17478, respectively.

<sup>1</sup>J. G. Bednorz and K. A. Müller, *Z. Phys. B* **64**, 189 (1986); M. K. Wu *et al.*, *Phys. Rev. Lett.* **58**, 908 (1987); R. J. Cava *et al.*, *ibid.* **58**, 1676 (1987); S. Uchida *et al.*, *Jpn. J. Appl. Phys.* **26**, L1 (1987).  
<sup>2</sup>L. F. Schneemeyer *et al.*, *Phys. Rev. B* **35**, 8421 (1987); Y. Yamaguchi *et al.*, *Jpn. J. Appl. Phys.* **26**, L447 (1987); R. L. Greene *et al.*, *Solid State Commun.* **63**, 379 (1987).  
<sup>3</sup>D. Vaknin *et al.*, *Phys. Rev. Lett.* **58**, 2802 (1987); T. Freltoft *et al.*, *Phys. Rev. B* **36**, 286 (1987).  
<sup>4</sup>S.-W. Cheong *et al.* (unpublished).  
<sup>5</sup>A. Schenck, *Muon Spin Rotation Spectroscopy: Principles and Applications in Solid State Physics* (Adam Hilger, Bristol, 1985).  
<sup>6</sup>Budnick *et al.* [*Europhys. Lett.* **5**, 651 (1988)] have recently obtained data similar to those on the right-hand side of Fig. 2.  
<sup>7</sup>Y. J. Uemura *et al.*, *Phys. Rev. Lett.* **59**, 1045 (1987); Budnick

*et al.*, *Phys. Lett. A* **124**, 103 (1987).

<sup>8</sup>R. S. Hayano *et al.*, *Phys. Rev. B* **20**, 850 (1979).

<sup>9</sup>A recent review of this subject is S. M. Shapiro *et al.*, *Physica B* **137**, 96 (1987).

<sup>10</sup>I. Watanabe *et al.*, *J. Phys. Soc. Jpn.* **56**, 3028 (1987); B. Batlogg (private communication); Y. Endoh *et al.* (unpublished).

<sup>11</sup>See, e.g., V. J. Emery, *Phys. Rev. Lett.* **58**, 2794 (1987).

<sup>12</sup>A. Aharony *et al.* (unpublished); G. Chen and W. A. Goddard III, *Science* **239**, 899 (1988); J. Zaanen and O. Gunnarsson (unpublished).

<sup>13</sup>G. Aeppli and D. J. Buttrey, *Phys. Rev. Lett.* (to be published).

<sup>14</sup>Reviews are contained in *Electron-Electron Interactions in Disordered Systems*, edited by A. L. Efros and M. Pollak (North-Holland, Amsterdam, 1985).